Bulletin of the Seismological Society of America, 92, 1, pp. 245–255, February 2002

The 1999 İzmit, Turkey, Earthquake: A 3D Dynamic Stress Transfer Model of Intraearthquake Triggering

by Ruth A. Harris, James F. Dolan, Ross Hartleb, and Steven M. Day

Abstract Before the August 1999 İzmit (Kocaeli), Turkey, earthquake, theoretical studies of earthquake ruptures and geological observations had provided estimates of how far an earthquake might jump to get to a neighboring fault. Both numerical simulations and geological observations suggested that 5 km might be the upper limit if there were no transfer faults. The İzmit earthquake appears to have followed these expectations. It did not jump across any step-over wider than 5 km and was instead stopped by a narrower step-over at its eastern end and possibly by a stress shadow caused by a historic large earthquake at its western end. Our 3D spontaneous rupture simulations of the 1999 İzmit earthquake provide two new insights: (1) the west- to east-striking fault segments of this part of the North Anatolian fault are oriented so as to be low-stress faults and (2) the easternmost segment involved in the August 1999 rupture may be dipping. An interesting feature of the İzmit earthquake is that a 5-km-long gap in surface rupture and an adjacent 25° restraining bend in the fault zone did not stop the earthquake. The latter observation is a warning that significant fault bends in strike-slip faults may not arrest future earthquakes.

Introduction

What Stops Earthquakes?

The question of what stops an earthquake remains unanswered. Some authors have proposed that strong sections of faults stop earthquakes (e.g., Aki, 1979), others have proposed that weak sections of faults stop earthquakes (e.g., Husseini *et al.,* 1975), and a third group has proposed that rather the nucleation process itself predetermines the eventual size of an earthquake (e.g., Ellsworth and Beroza, 1995). Yet another possibility is that fault geometry helps determine the rupture process (e.g., Wallace, 1970; Segall and Pollard, 1980; Sibson, 1985, 1986; Harris *et al.,* 1991). In this article we examine the theoretical studies of fault geometry affecting earthquake size and compare the predictions with what actually occurred during the 1999 İzmit, Turkey, earthquake.

Previous Geological Observations and Numerical Studies of Earthquakes and Step-Overs

The geometrical complexity of faults has been observed in the field by geologists for decades (e.g., Wallace, 1970; Segall and Pollard, 1980) and more recently inferred by seismologists examining detailed wave recordings (Li *et al.,* 1994) and precise aftershock relocations (Felzer and Beroza, 1999). Speculations about the behavior of earthquakes near one type of geometrical complexity, the step-over (Fig. 1), are based on a worldwide compilation of predominantly geological data (e.g., Sibson, 1985, 1986; Knuepfer, 1989). Some of the observations are from previous earthquakes in Turkey, including the great Erzincan earthquake of 1939 (Barka and Kadinsky-Cade, 1988; Wesnousky, 1988). Barka and Kadinsky-Cade (1988) proposed that 5 km may be the widest step-over that can be jumped by an earthquake.

How these fault complexities physically affect earthquake rupture is best understood through numerical modeling of simulated earthquakes encountering these changes in fault geometry. The numerical models need to be fully dynamic and include the waves generated by an earthquake. Harris *et al.* (1991) undertook such a study and examined the effect of a fault step-over on a propagating rupture in two dimensions. Kase and Kuge (1998) performed a similar study and also examined the case of perpendicular faults. Modeling efforts were expanded in 1993 to include the effects of pore fluids (Harris and Day, 1993) and in 1999 to encompass three dimensions, including fault depth and the Earth's free surface (Harris and Day, 1999). Although the studies were highly simplified pictures of faulting and assumed that the Earth's crust behaves elastically near a fault, they did make predictions about the behavior of an earthquake near a step-over. These predictions included the significance of fault depth (width) and length, the width and amount of overlap of the step-over (Fig. 1), and the impact of previous earthquake history. One important assumption in the step-over simulations is that the faults do not intersect at depth and that there are no transfer faults such as the Kickapoo (Landers) fault that slipped during the 1992 M_w

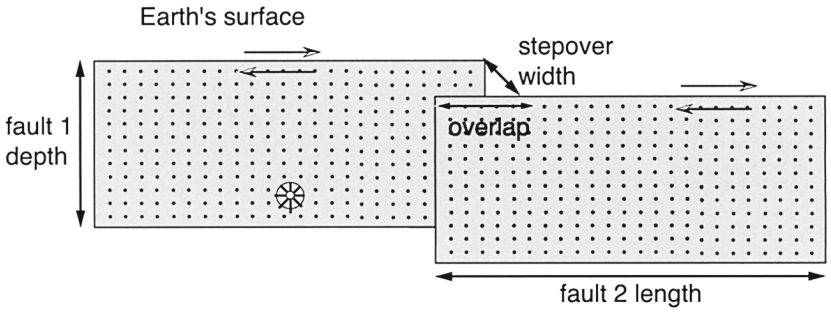

Figure 1. En-echelon vertical strike-slip faults. A right step in a right-lateral strike-slip fault is a dilational step-over (depicted). A left step would be a compressional step-over. The perpendicular distance between the two faults is the step-over width, and the overlap distance is measured along-strike. The simulated earthquake is artificially nucleated in a region, denoted by the star on the first fault plane, and is not forced, but is allowed to propagate spontaneously. Whether the earthquake can jump across the step-over between the faults depends on the fault geometry and the stress conditions on the two faults.

7.3 Landers, California, earthquake (Sieh *et al.,* 1993; Sowers *et al.,* 1994). That transfer or linking faults can enable ruptures to jump across step-overs that are wider than those jumped by ruptures on unlinked faults was proposed by Harris and Day (1993) for strike-slip faults and Magistrale and Day (1999) for simulated thrust faults.

The Method

We use a 3D finite-difference computer program to simulate a strike-slip earthquake encountering multiple noncollinear fault segments. The general methodology for our spontaneous rupture simulations in a 3D medium is the same as that explained by Day (1982). The computer program is the same as that used by Harris and Day (1999), where unlike Day (1982), there is more than one fault present and a free surface that represents the Earth's surface is included.

In our numerical simulations, we ensure that our results are not contaminated by waves returning from the edges of our finite-difference grid by setting the edges sufficiently far from the modeled fault segments. We also use a damping parameter within the finite-difference grid to suppress short-wavelength dispersion. Aside from the faults themselves, the medium is assumed to be linearly elastic. The simulated earthquake is artificially nucleated over a small area (Day, 1982) on the first fault segment and then allowed to spontaneously propagate on that fault segment. Spontaneous propagation implies that the rupture is not forced to travel at a prescribed velocity, but instead its velocity is determined by the stress conditions on the fault segment(s) at each point in time. The rupture continues to propagate as long as there is enough available fracture energy. If there is a step-over at the end of the first fault segment, there are three possibilities: (1) the rupture does not have enough energy to make the jump to a second fault segment and stops at the step, (2) the rupture has just enough energy to jump across the step but not enough to continue propagating on the second fault segment, and (3) the rupture has enough energy to jump the step and to continue propagating on the second fault segment. The third option leads to the largest earthquake because the rupture length is the longest. Whether the rupture is able to jump the step-over and continue propagating on the next fault segment depends on the stress conditions on both sides of the step. Harris and Day (1999) found cases where one simulated earthquake might not make a jump, but the next simulated earthquake in a sequence did jump across the same step-over. The only difference between the two simulated earthquakes was the set of initial stress conditions for each fault segment. For the second event, these stresses were the summed effect of the static stress changes due to the first event and the increment in tectonic load accumulated on the faults during the time between the earthquakes.

Slip-Weakening Fracture Criterion

To determine when a point on a fault segment may slip during the rupture process, we incorporate a slip-weakening fracture criterion (Ida, 1972; Andrews, 1976a,b; Day, 1982) (Fig. 2). This fracture criterion is similar to the Coulomb criterion often used in static stress change studies (see review article by Harris, 1998), except that for slip-weakening the coefficient of friction, μ, is a function of fault slip, d, and since we are dealing with a dynamic problem, the shear and normal stresses are time dependent. Failure can occur when the time-dependent shear stress, $\tau(t)$, exceeds the slip-dependent coefficient of friction, $\mu(d)$, multiplied by the time-dependent normal stress, $\sigma(t)$, plus cohesion, c:

$$\tau(t) > (\mu(d)\sigma(t)) + c. \quad (1)$$

The slip-weakening fracture criterion, which helps smooth the rupture tip and prevent runaway rupture propagation, is inferred from laboratory experiments (Dieterich, 1981) and is consistent with seismic observations (Day *et al.,* 1998). We use a slip-weakening critical distance, d_0, of 20 cm, but the results do not change significantly if we change the value by 10 cm. The cohesion parameter, c, outside the fault segments is set to a very high value so that the rupture will not extend beyond these segments. On the fault segments themselves, the cohesion, c, is set to zero.

The Model

In this article, we model the M_w 7.4 Kocaeli (İzmit), Turkey, earthquake that occurred on the North Anatolian

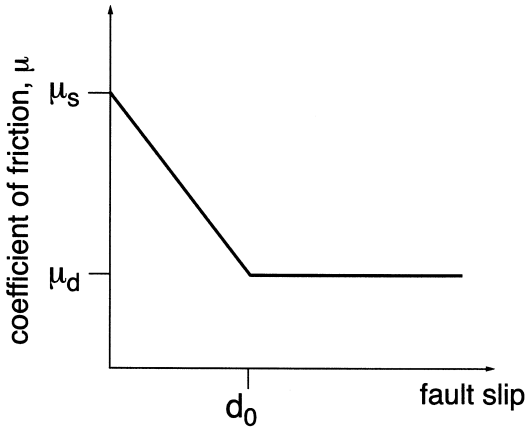

Figure 2. The slip-weakening fracture criterion (Ida, 1972; Andrews, 1976a,b; Day, 1982) determines when the fault can slip. The strength of a point on the fault is proportional to the time-dependent normal stress, with the proportional factor being the coefficient of friction, μ, which is determined by how much slip has occurred at that point. Initially, before any slip has occurred, μ equals μ_s, the static coefficient of friction. When the fault starts to slip, μ linearly decreases until the fault has slipped a distance called the critical distance, d_0. After the fault has slipped d_0, μ equals μ_d, the dynamic, or sliding friction. Table 1 lists the values of μ that we used in our simulations.

fault system in August of 1999. We use the geologically mapped onshore and seismologically mapped offshore surface trace of the 1999 İzmit earthquake to estimate the fault segment lengths, step-over widths, and fault segment overlaps for our numerical simulations (Fig. 3). We model four fault segments, representing, from west to east, the Karamürsel (east of Yalova to Gölcük), Sapanca (Gölcük-Lake Sapanca), Sakarya (Lake Sapanca-Akyazi), and Karadere (Akyazi-Eften Lake) segments (Barka, 1999; Fumal *et al.,* 1999; Hartleb *et al.,* 1999, 2002; Parke *et al.,* 1999; I. Kusçu, 2001, unpublished results; Okay *et al.,* 2000; U.S. Geological Survey, 2000; Langridge *et al.,* 2002). The Karamürsel, Sapanca, and Sakarya segments are assumed to be parallel, with a strike of 90° NE, and the Karadere segment is assigned a strike of 67.5° NE. All the fault segments are assumed to be vertical with depths extending from the Earth's surface down to 15 km.

The August 1999 earthquake appears to have originated on the 40-km-long Sapanca segment, east of a 1- to 2-km-wide right (dilational) step-over near the city of Gölcük (Ito *et al.,* 1999; Honkura *et al.,* 2000; M. Aktar, personal comm., 2000). A prominent normal fault in the step-over slipped by approximately 2 m during the earthquake, and we infer that this fault links the two sides of the step-over, providing a continuous mechanical connection between the Karamürsel segment to the west and the Sapanca segment to the east. Because our finite-difference computer program cannot perfectly represent the dipping normal fault, we model the normal fault as a series of short parallel strike-slip faults that can accommodate the transfer of motion, or as a dilational step-over. We infer there is no overlap and there is a 1- to 2-km-wide right (dilational) step-over between the Sapanca and the 26-km-long Sakarya segments (Lettis *et al.,* 2000; R. Witter and W. Lettis, personal comm. 25 January 2000). Because the details of the step-over are under Lake Sapanca, the exact amount of overlap and step-over width was not known at the time this article was written. The Sakarya segment contains a 1-km-wide left (compressional) step-over with no overlap approximately 20 km east of Lake Sapanca (Fumal *et al.,* 1999; U.S. Geological Survey, 2000). We include this left step in our model of the Sakarya segment. Between the Sakarya and the Karadere segments, there is a 5-km gap in the surface rupture (Hartleb *et al.,* 1999, 2002). We assume that this gap extends throughout the seismogenic zone, although future studies may show evidence for the continuation of the faulting at depth. The Karadere segment trends more northeasterly and shows an approximately 22.5° change in strike from the eastern end of the Sakarya segment. The eastern end of the August earthquake was on the 22-km-long Karadere segment, where the rupture terminated in a series of en-echelon faults within a diffuse right step-over (Hartleb *et al.,* 1999, 2002). Our finite-difference computer program cannot exactly model the spontaneous rupture propagation from the west–east-striking faults to the northeasterly striking Karadere segment, so we make an approximation. We let the rupture spontaneously propagate on the west–east-striking faults and save the time-dependent stress waves caused by this rupture at the site of and in the coordinate system of the northeasterly striking Karadere fault segment. We then restart the simulation as a stand-alone spontaneous rupture on the Karadere segment but include the time-dependent stress waves generated by the west–east-striking faults, in addition to those generated by the spontaneous rupture on the Karadere segment itself. This approximation should be accurate for the spontaneous rupture propagation on the Karadere segment. The only feature that we might conceivably miss is the effect of the Karadere-generated stress waves on subsequent slip of the fault segment west of the Karadere, the Sakarya segment.

Recent marine geophysical data obtained near the western end of the rupture indicate that the North Anatolian fault is a continuous west-trending fault from Gölcük to just east of Yalova (see Fig. 3a). In contrast, earlier interpretations of the fault in this region have suggested the presence of a step-over in the fault near the eastern edge of the Hersek penninsula (Barka, 1999; Lettis *et al.,* 2000; R. Witter and W. Lettis, personal comm. 25 January 2000). Although the recent data suggest that the active fault has no step-over at this location, for the sake of completeness, we have also tested the behavior of the simulated rupture encountering a 4- to 5-km-wide step-over near Karamürsel, as proposed by Lettis *et al.* (2000). Although the pattern of aftershocks did continue much farther west than the Hersek penninsula, estimates from Global Positioning System (GPS) and interferometric synthetic aperture radar (InSAR) measurements

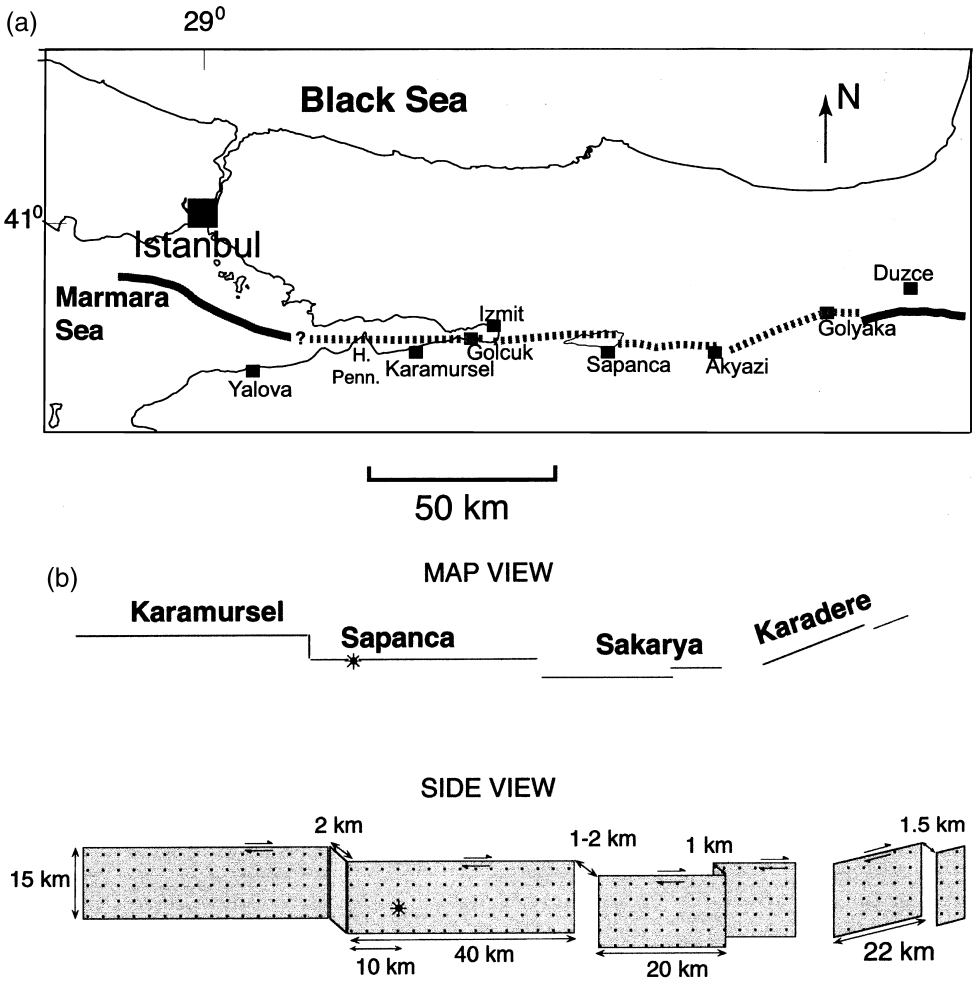

Figure 3. (a) Location of the 1999 İzmit earthquake rupture in Turkey is shown by the dashed gray fault segments (figure is modified from Barka, 1999; Parke *et al.,* 1999; Kuşçu *et al.,* 2000; Okay *et al.,* 2000). The eastern solid dark gray fault segment shows the part of the North Anatolian fault that ruptured in the November 1999 *M* 7.2 Düzce earthquake. The western solid dark gray fault segment striking toward Istanbul is called the Princes Island strand of the North Anatolian fault. This portion of the fault probably did not rupture in 1999. The question mark indicates that we do not know exactly how the Karamürsel fault segment connects to the Princes Island strand. H. Penninsula is the Hersek penninsula. The squares show locations of cities. (b) We use a simplified version of the coseismically active fault trace mapped by the geologists and inferred by the geodesists (Fig. 3a) and assume that the faults are primarily west–east-trending and extend vertically from the Earth's surface down to 15-km depth. The Karadere segment is assigned a 22.5° change in strike from the other faults to the west. The simulated earthquake nucleates on the Sapanca segment, at 9-km depth, following the seismological observations.

recorded both before and after the earthquake indicate that the rupture stopped at or east of 29.5° longitude, the location of the Hersek delta (Reilinger *et al.,* 2000b), or maybe continued 10–15 km farther west, but with less than 2 m of slip (Reilinger *et al.,* 2000a; Wright *et al.,* 2001).

Preliminary seismological models of the İzmit earthquake based on a local network that recorded the earthquake have placed the hypocenter of the earthquake at about 9 km depth, just east of the İzmit Bay at 29.955° latitude, 40.724° longitude (M. Aktar, personal comm. to Bill Ellsworth, 15 February 2000), so this is where we nucleate our simulated earthquake. In our first simulations we set the initial principal stress conditions to be equal for all of the fault segments. Subsequently, we examine heterogeneous conditions.

Results

We tested a variety of initial stress conditions, as the actual values are not known in the Earth's crust (Table 1). We start with homogeneous initial stress conditions, loosely based on those suggested by McGarr (1984) for midcrustal

Table 1
Initial Stress Conditions

Name	Initial Shear Stress (MPa)	Initial Normal Stress (MPa)	μ_s	μ_d	Initial Stress Drop (MPa)
High-stress far from failure	70.00	−120.0	0.667	0.525	7
Low-stress far from failure	22.75	−30.00	1.133	0.525	7
High-stress close to failure	70.00	−120.0	0.613	0.525	7
Low-stress close to failure	22.75	−30.00	0.875	0.525	7

depths, then examine other possible conditions, both homogeneous and heterogeneous, to discover which one of them might allow the simulated earthquake to rupture the fault segments that slipped during the actual earthquake. In all of the simulations, the İzmit rupture nucleates at 9-km depth on the Sapanca segment and then propagates outward on that fault segment (Fig. 3). In our initial tests, the step-over width between the Sapanca and Sakarya segments is assumed to be 1 km. We also test a 2-km-wide step-over because the actual step-over width at depth is unknown at the time this article was written. Hopefully, future earthquake relocation studies will elucidate the true width.

A successful simulation reproduces the following observations: on the western side of the hypocenter, the simulated earthquake reaches the step-over between the Sapanca and Karamürsel segments, and as the fault segments are connected, the rupture easily transitions itself to the Karamürsel segment. The rupture reaches almost to the western end of the Karamürsel segment, where it terminates. Meanwhile, the bilateral rupture is propagating eastward and updip to reach the Earth's surface. The rupture transitions across the dilational (right) step-over between the Sapanca and Sakarya segments, jumps the compressional (left) step-over on the Sakarya segment, and reaches the end of the Sakarya segment. The 5-km gap and the 22.5° change in strike to the Karadere segment do not stop the rupture but allow it to continue propagating, although surface slip is reduced to 1–2 m. At the eastern end of the Karadere segment the rupture jumps a 1- to 2-km-wide step-over and then stops.

One-Kilometer-Wide Sapanca Lake Step-Over

We first examine the case of a 1-km-wide step-over between the Sapanca and Sakarya segments. We start with tests of both low (e.g., normal stress = −30 MPa) and high (e.g., normal stress = −120 MPa) initial stress conditions and a 7-MPa initial stress drop (Table 1). The initial stress drop is equal to the initial shear stress minus the dynamic coefficient of friction, μ_d, multiplied by the initial normal stress. We find that the simulated earthquake cannot propagate across the 1-km-wide Sapanca Lake step-over (or any of the other step-overs) if the initial stresses are high and far from failure. (When we use the term "far from failure," we are referring to the difference between the initial and failure stress relative to the stress drop. The term "far from failure" indicates that this ratio is larger, whereas "close to failure" indicates that this ratio is smaller). This result of a high-stress, far-from-failure fault not being able to jump a 1-km-wide step-over is the same result as that presented in the generic models of Harris and Day (1999). If the initial stresses are instead low, but the faults are still far from failure, the 1-km step-over at Sapanca Lake is jumped (although a 2-km-wide Sapanca Lake step-over is not), but the transition to the Karamürsel segment is difficult. This case also results in unlikely triggering of the Karadere segment.

Simulations that better match the observations seem to require that the west–east faults be close to failure (Table 1). High-stress, close-to-failure conditions allow jumping of the narrow (<5 km wide) steps, as do low-stress, close-to-failure conditions. In both high-stress, close-to-failure and low-stress, close-to-failure situations, the simulated earthquake can jump the narrow (<5 km wide) step-overs and propagate along the entire Sapanca, Sakarya, and Karamürsel fault segments. Figure 4 shows the simulated earthquake for the low-stress, close-to-failure case.

Although new marine geophysical data show that there is no step-over within the Karamürsel segment (e.g., Kusçu *et al.,* 2000), other authors (e.g., Barka, 1999; Lettis *et al.,* 2000) have proposed a step-over from a Karamürsel segment that extends from just west of Karamürsel to Golçuk, to a Yalova segment that starts just west of Karamürsel, skirts the northern tip of the Hersek penninsula, and continues westward. Therefore, we also simulated the case of a 3- to 5-km-wide step-over east of the Hersek penninsula, between the Karamürsel and Yalova segments proposed by the other authors. We find that if a 4-km-wide step-over existed east of the Hersek penninsula, the rupture might not have been able to jump the step-over, whereas if the hypothetical step-over were 3 km wide or less, the rupture might have been able to jump the step-over and continue westward.

In this article, we use the fault segmentation models that show no step-over in the North Anatolian fault from Golçuk to west of the Hersek penninsula (Fig. 3a). Therefore, as our initial stress conditions have been assumed to be homogeneous on the fault segments, the rupture has no trouble propagating to the west beyond the Hersek penninsula. Also, the simulated earthquake has no trouble producing large amounts of slip on the Karamürsel segment that exceed those inferred from geodetic observations (Reilinger *et al.,* 2000a,b; Wright *et al.,* 2001). We will return to address this issue and propose an explanation for the western termination of the August 1999 earthquake.

Dynamic Triggering of the Karadere Segment

To satisfy the observations, the simulated rupture also needs to propagate along the Karadere segment. This implies that unlike our previous simulations of parallel strike-slip

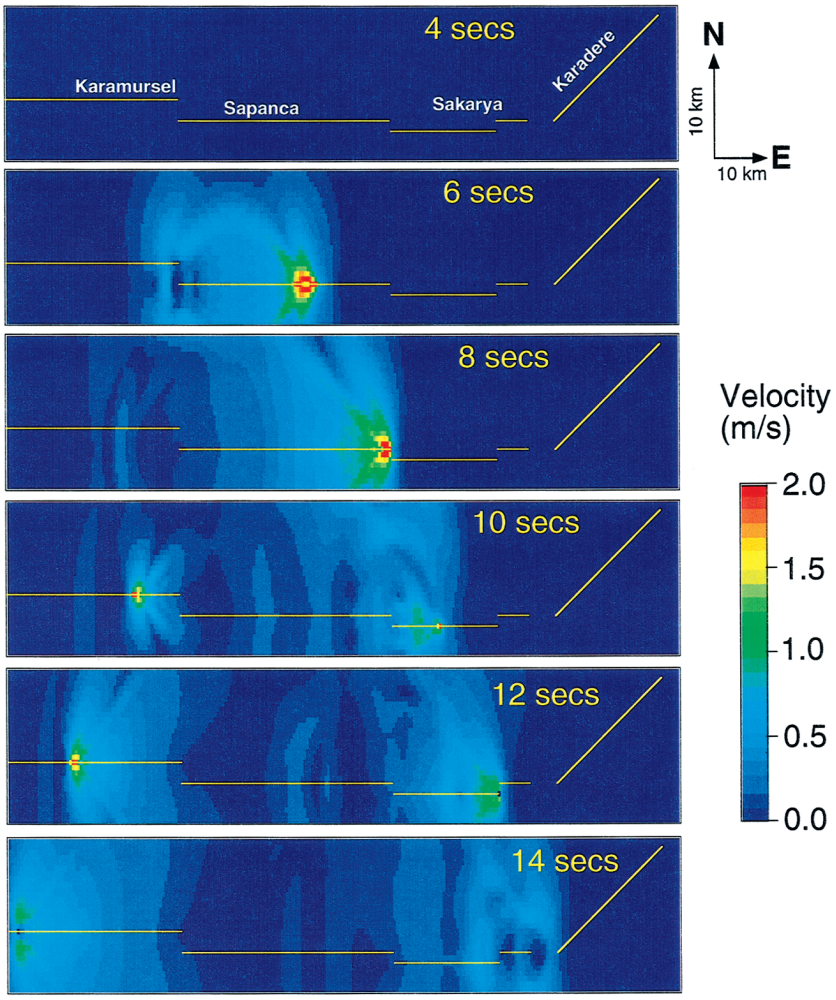

Figure 4. The slip velocities at the Earth's surface resulting from a simulated earthquake that nucleates at 9-km depth along the Sapanca segment and then spontaneously propagates. In this example the step-over width at Sapanca Lake is assumed to be 1 km wide. At 4 sec after nucleation, the rupture has not yet made it to the Earth's surface but is propagating at depth in the updip, downdip, and along-strike directions on the Sapanca segment. At 6.04 sec the rupture makes the jump at the Earth's surface from the Sapanca to the Karamürsel segment (in this case there is no transfer fault). The rupture continues its progression westward on the Karamürsel segment and propagates until it reaches the (western) end of the Karamürsel segment. To the east, the rupture jumps to the Sakarya segment at depth at 8.08 sec and at the Earth's surface at 8.64 sec. The rupture jumps the compressional step-over within the Sakarya segment at 12.20 sec. The Karadere segment is first triggered at 14.16 sec (not shown in this figure).

faults (e.g., Harris and Day, 1999) where we only needed to know the value of σ_{zz}, the stress that acts normal (perpendicular) to the west–east direction, we now also need to know the value of σ_{xx}, the stress that acts normal to the north–south direction. We need to determine if there are reasonable values of the initial shear and normal stresses that will allow rupture propagation from the west–east-striking fault segments to the east–northeast-striking Karadere segment, a restraining (compressional) bend. A rupture on the west–east fault segments increases the normal stress on the Karadere segment, so a large initial shear stress, arising from large σ_{xx}, is needed to permit any jump to the Karadere segment. With the large dynamic compressive stress and the same static to dynamic friction drop that we have assumed for the rest of the fault segments (Table 1), large dynamic stress drops result. Large dynamic stress drop can, in turn, produce a very large slip on the Karadere segment, whereas at least at the Earth's surface, geologists did not observe any large slip. What are the appropriate initial stress values that allow the rupture to jump to the Karadere segment and that also reproduce the geologically observed surface slip on the Karadere segment? Here are two of the possibilities that we examined and their outcomes—(1) For the high-stress, close-to-failure situation (Table 1), we find that rupture of the modeled Karadere segment is not possible unless σ_{xx} is an extremely (unrealistically) high value, of the order of -320 MPa. This implies that although the high-stress, close-to-failure situation was sufficient for jumping the step-overs in the west–east-striking faults, it produces problems for Karadere triggering. (2) For our favored low-stress, close-to-failure situation (Table 1) we have to assume σ_{xx} to be of the order of -130 MPa to achieve failure of the Karadere segment. Although these values ($\sigma_{zz} = -30$ MPa, $\sigma_{xx} = -130$ MPa) led to almost realistic principal stresses and principal stress directions for this part of the North Anatolian fault, they also led to an excess of slip (>5–10 m) over the entire Karadere segment. This amount of seismic moment on the Karadere segment has not been deduced for the actual earthquake.

At the Earth's surface, the geologically determined surface slip values are of the order of 1–2 m (Hartleb *et al.,* 1999, 2002). A model derived from GPS data shows 1–2 m of slip on the upper portions of the Karadere segment (Reilinger *et al.,* 2000a). Seismological models show more slip

at depth. A kinematic model derived by inverting strong-motion data, with the constraint of the measured surface slip (Bouchon *et al.,* 2000), and a kinematic model derived by a joint inversion of strong-motion, teleseismic, and InSAR data, with the constraint of the measured surface slip (Delouis *et al.,* 2002), show a high-slip patch at depth, with a fault-plane average of less than 3 m slip. Therefore, although it is permissible to have high slip at depth, the spontaneous rupture model of the Karadere segment should show a lesser amount of slip near the Earth's surface and concur with the geological slip measurements. In subsequent sections of this article we address possible solutions to this dilemma.

Heterogeneous Stress Conditions: Stress Changes Caused by Previous Earthquakes

Previous earthquakes near the 1999 İzmit earthquake may have affected the stress conditions on the faults that ruptured during the İzmit earthquake (e.g., Stein *et al.,* 1997; Nalbant *et al.,* 1998; Hubert-Ferrari *et al.,* 2000; Parsons *et al.,* 2000). We therefore attempt to include the effect of past earthquakes in our dynamic rupture models. The twentieth century earthquakes that make the most difference for the easternmost İzmit fault segments are the 1967 M_s 7.1 Mudurnu earthquake and the 1943 M_s 6.4 Hendek–Adapazari earthquake (Nalbant *et al.,* 1998; Barka, 1999). Both these earthquakes occurred within 20 km of the 1999 İzmit earthquake, with the location of the 1967 event much better constrained than the 1943 event (Fig. 5). Simple dislocation models of these pre-İzmit events are calculated to have modified the static stresses east of Sapanca Lake by approximately 0.1 MPa (T. Parsons, personal comm. May 2000). When we simulate the 1999 İzmit earthquake using these modified initial stress conditions east of the Sapanca Lake, we find a similar result to that without the static stress changes caused by the two previous earthquakes. This is because the 0.1-MPa static stress changes produced by the 1943 and 1967 earthquakes are unable to counteract the dynamic stress changes of 1–3 MPa that occur during the simulated İzmit earthquake.

Also of interest is what stopped the 1999 İzmit earthquake at its western end, as mentioned previously. We now discuss the possible role of previous earthquakes in the vicinity. Other studies (e.g., Lettis *et al.,* 2000) have proposed that a 4- to 5-km-wide step-over within the Karamürsel segment stopped the rupture east of the Hersek penninsula. However, recent marine seismic studies show that there is no step-over within the Karamürsel strike-slip segment (e.g., Kusçu *et al.,* 2000), and Wright *et al.* (2001) infer an İzmit rupture termination 10–15 km west of the Hersek Penninsula (Figs. 3a and 5). Therefore, it is still unclear what slowed down and then stopped the İzmit earthquake as it propagated westward.

An examination of the earthquake history near İzmit provides one possible explanation. The large M_S 7.3 1894 earthquake on the North Anatolian fault may have ruptured the same westernmost fault segment (Ambraseys, 2001; Ambraseys and Jackson, 2000) as the August 1999 İzmit earthquake (Fig. 5). This would have resulted in the 1999 earthquake encountering portions of the North Anatolian fault that were not primed for rerupture. That is, long-term tectonic loading of the Karamürsel fault segment, particularly the western part of that segment, would not yet have eroded

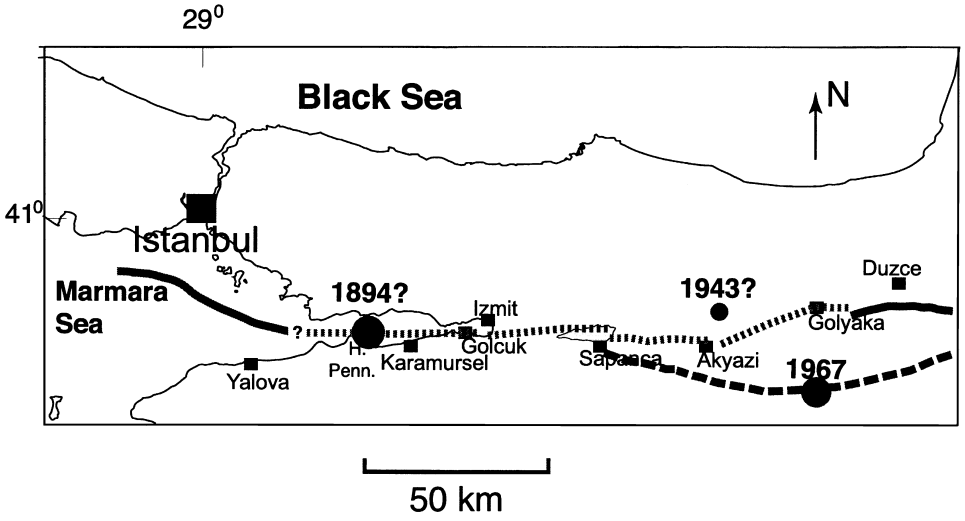

Figure 5. The 1943 Hendek-Adapazari and 1967 Mudurnu earthquakes occurred close to the 1999 İzmit earthquake, but the exact location of the 1943 earthquake is poorly known (Nalbant *et al.,* 1998). (Figure modified from Barka, 1999; Parke *et al.,* 1999; Kusçu *et al.,* 2000; Okay *et al.,* 2000.) The 1894 earthquake occurred in the Marmara Sea (Ambraseys, 2001; Ambraseys and Jackson, 2000) and may have affected the westward rupture extent of the 1999 İzmit earthquake. H. Penn. is the Hersek penninsula.

the 1894 stress shadow (i.e., stress decrease; see Harris and Simpson [1998] for further discussion about stress shadows). Although the static stress changes caused by the 1943 and 1967 earthquakes were not efficient at hampering the propagation of the 1999 İzmit earthquake in the east, as the 1943 and 1967 earthquakes were relatively far away from the 1999 fault segments, the 1894 earthquake would have had much more of a stress shadow impact (e.g., 1–10 MPa) had it occurred at a distance of 0 km from the 1999 earthquake. We therefore propose that the 1999 earthquake may have stopped just west of the Hersek penninsula because it was unable to overcome the stress shadow (stress decrease) generated by the 1894 event.

Discussion

We have found a set of homogeneous initial stress conditions that would have permitted rupture of the fault segments that ruptured during the 1999 İzmit earthquake. The slips produced by this model, with the exception of the Karadere segment, are not very different from the geologic slip measurements made at the Earth's surface (e.g., USGS, 2000), or the slip inferred from the GPS data (Reilinger *et al.,* 2000a). The spontaneous rupture model is also more or less consistent with the seismologically inferred slip (e.g., Bouchon *et al.,* 2000; DeLouis *et al.,* 2002), although there are still some questions to resolve about the seismological data, as the seismological models vary in their opinions about rupture velocity and final slip distribution. One consistent feature that we were unable to explain with the homogeneous initial stress model, or even with a very simple model that includes previously inferred locations for the 1943 and 1967 earthquakes, is the amount of slip on the Karadere segment. Our models greatly overpredict the amount of surface slip on this fault segment, where only 1–2 m of slip was observed.

The 1943 Earthquake

One potential explanation for the mismatch on the Karadere segment is the 1943 Hendek–Adapazari earthquake. The location of the 1943 earthquake is not well determined (Nalbant *et al.*, 1998). We examined the possibility that the 1943 earthquake occurred much closer to the Karadere segment than assumed by previous authors, possibly on the Karadere segment itself. If this is the case, then the static stress changes caused by the 1943 earthquake on the Karadere segment would have been much greater than the previously estimated 0.1 MPa. When we modify the initial stress conditions in the spontaneous rupture model of the 1999 earthquake to include a close-in 1943 earthquake, we still find it difficult to produce reasonable surface slip values on the Karadere segment. This is because a σ_{xx} value of -130 MPa is still required to trigger the Karadere segment in the first place, resulting in a fault segment that is very close to failure. We now examine two other possibilities for explaining the slip on the Karadere segment: the coefficient of friction and the possibility of nonvertical fault dip.

Low-Friction Faults?

One approach to achieving easier rupture of the Karadere segment is to lower the coefficient of friction in our fracture criterion. Our current static coefficient is 0.875 for the close-to-failure cases (Table 1). If the Karadere segment had experienced an earthquake more recently than the other (west–east) fault segments, one might expect that it would not have had as much time to heal, or regain its strength, so its coefficient of friction might be lower (D. Lockner, personnel comm. July 2000). Unfortunately, we cannot resort to this approach solely for the Karadere segment because we have no evidence that the Karadere segment did rupture more recently than its west–east-striking counterparts. Therefore, we examine instead a systemwide lowering of the coefficient of friction to determine if this can help solve the conundrum.

We keep the stress drop at 7 MPa and the normal stress at 30 MPa and examine cases where μ_d is 0.1, μ_s is 0.4–0.5, and the shear stress is 10 MPa. The main objective is to see if these new parameters will allow a smaller value of σ_{xx} and thereby a smaller stress drop on the Karadere segment. The result is that a smaller surface slip does occur on the simulated Karadere segment, although it is still of the order of 5 m, a factor of 2 to 3 greater than the observed surface slip.

A Dipping Karadere Segment?

In all of the aforementioned simulations, we have assumed that the faults are vertical. Rupture around a compressional bend could be facilitated by a nonvertical dip, so we examined the range of dips that might allow for a lower σ_{xx} value, leading to a smaller stress drop and thereby less slip on the Karadere segment. In our finite-difference computer program, we are not able to explicitly model a spontaneous rupture that starts on a vertical fault, and then transitions into a dipping fault striking in another direction. Instead we have done a much simpler static stress calculation, examining a range of σ_{xx} values (0 to -100 MPa) and Karadere segment dips (45°–85°). For our other parameters we employ the low-stress, close-to-failure values used before (Table 1); σ_{zz} is -30 MPa, μ_s is 0.875, and stress drop is 7 MPa. We find that a dip of 60° would allow the magnitude of σ_{xx} to decrease to -70 MPa and a dip of 45° could permit σ_{xx} to be equal to -50 MPa. Both these dips would lead to lower stress drops on the Karadere segment, yet permitting triggering of this segment. A 60° dip is not inconsistent with the inversions of the InSAR data for a six-segment İzmit rupture model. Wright *et al.* (2001) show their İzmit static slip model allowing a dip of 61° for the Karadere segment, although the resolution of the easternmost portion of the fault may not be ideal.

An intermediate possibility might be that the Karadere

segment is close to vertical near the Earth's surface, as revealed by the geological slip measurements (Hartleb *et al.*, 2002), but dips shallowly at 10–15 km depth. This conclusion is, at the present time, highly speculative, and further analysis of aftershock data near the Karadere segment may help clarify the situation (N. Seeber, personnel comm. August 2000). Additional illumination on the details of the dip of the Karadere segment could, in the future, be provided by gravity surveys in the vicinity of the Karadere segment (C. Nicholson, personnel comm. August 2000). One possible clue may lie in the determination of the kinematics between the Karadere and Düzce segments of the North Anatolian fault. For example, the western part of the Düzce segment, which lies just east of the Karadere segment, ruptured in a large earthquake that occurred in November 1999 and appears to have dipped at 50°–60° (Bürgmann *et al.,* 2002).

Other Complexities and Findings from Our Simple Models

In our aforementioned studies we have ignored some major known complexities in the Earth's structure, such as the inhomogeneous velocity structure of the crust surrounding the North Anatolian faults and the true geometrical complexities of the faults. We have also been unable to model unknown complexities in the stress field, such as the exact orientations of the principal stress directions in the vicinity of each of the fault segments from the Marmara Sea to Akyazi. Moreover, the stress conditions that might result from the history of previous earthquakes on these fault segments are also unresolved. We could, in theory, include all of these complexities in our models, if the details were known. Perhaps this is a fruitful exercise for the future, when the fine structure of the fault geometry and rocks at depth and stresses both at depth and near the Earth's surface along the North Anatolian fault are better understood.

Even with our very simple models of the August 1999 earthquake we are able to come to some significant conclusions. One of the interesting features of the İzmit earthquake is that it propagated across fault steps and bends. If these features extend in depth as a continuation of their surface expression, the geometrical complexity may provide an insight into the absolute stress levels on the fault. For example, if the step-overs are 1–2 km wide at depth and the bend to the Karadere segment extends to depth, it appears that high levels of resolved stresses (shear and normal stresses) on the west–east-striking segments are insufficient to permit the observed rupture propagation. Instead, the west–east-striking segments (Sapanca, Sakarya, and Karamürsel) may be lower stress faults. This hypothesis merits future study and may, perhaps, be evaluated with a thorough investigation of the foreshock and aftershock focal mechanisms on the İzmit rupture surface.

An important observation from the 1999 İzmit earthquake is that a major bend in the North Anatolian fault did not stop the earthquake. This concept of bends not stopping strike-slip earthquakes was proposed by Barka and Kadinsky-Cade (1988) for strike-slip earthquakes in general, and the İzmit earthquake is a reminder. Therefore, future earthquake hazard maps and earthquake probability studies should not use less than 30° bends to segment strike-slip faults.

Conclusions

We have presented a 3D spontaneous rupture model for the 17 August 1999 İzmit, Turkey, earthquake. This earthquake jumped narrow step-overs, jumped across a slip gap, and propagated around a bend before terminating. The range of geometrical features encountered by this earthquake may provide us with some bounds on the stress state of the North Anatolian fault in western Turkey. It appears that in the region of the 1999 İzmit earthquake, much of the fault is oriented as a low-stress fault. The İzmit earthquake also serves to remind us that significant fault bends may not arrest a propagating earthquake.

Acknowledgments

Thanks to Roland Bürgmann for his very thoughtful discussions about the geodetic slip models, Nano Seeber for the very enlightening discussions about the Karadere segment, Bill Lettis, Shinji Toda, Tom Parsons, and Ross Stein for their helpful discussions about the western extent of the İzmit earthquake, and Bill Ellsworth and Nobuo Hurukawa for originally guiding us to the hypocenter information. Joe Andrews pointed out that dipping faults allow ruptures to propagate around bends. Roland Bürgmann, Michel Bouchon, and Bertrand Delouis kindly shared their kinematic models of the İzmit earthquake before publication. Joan Gomberg provided a very helpful internal review. Joe Andrews and Liz Hearn provided very helpful external reviews. This is SCEC Contribution No. 595.

References

Aki, K. (1979). Characterization of barriers on an earthquake fault, *J. Geophys. Res.* **4,** 6140–6148.

Ambraseys, N. (2001). The earthquake of 10 July 1894 in the Gulf of İzmit (Turkey) and its relation to the earthquake of 17 August 1999, *J. Seism.* **5,** 117–128.

Ambraseys, N. N., and J. A. Jackson (2000). Seismicity of the Sea of Marmara (Turkey) since 1500, *Geophys. J. Int.* **141,** F1–F6.

Andrews, D. J. (1976a). Rupture propagation with finite stress in antiplane strain, *J. Geophys. Res.* **81,** 3575–3582.

Andrews, D. J. (1976b). Rupture velocity of plane strain shear cracks, *J. Geophys. Res.* **81,** 5679–5687.

Barka, A. (1999). The 17 August 1999 İzmit earthquake, *Science* **285,** 1858–1859.

Barka, A. A., and K. Kadinsky-Cade (1988). Strike-slip fault geometry in Turkey and its influence on earthquake activity, *Tectonics* **7,** 663–684.

Bouchon, M., N. Toksöz, H. Karabulut, M.-P. Bouin, M. Dietrich, M. Aktar, and M. Edie (2000). Seismic imaging of the İzmit rupture inferred from the near-fault recordings, *Geophys. Res. Lett.* **27,** 3013–3016.

Bürgmann, R., M. E. Ayhan, E. J. Fielding, T. J. Wright, S. McClusky, B. Aktug, C. Demir, O. Lenk, and A. Türkezer (2002). Deformation during the 12 November 1999 Düzce, Turkey, earthquake, from GPS and InSAR data, *Bull. Seism. Soc. Am.* **92,** no. 1, 161–171.

Day, S. M. (1982). Three-dimensional simulation of spontaneous rupture: the effect of nonuniform prestress, *Bull. Seism. Soc. Am.* **72,** 1881–1902.

Day, S. M., G. Yu, and D. J. Wald (1998). Dynamic stress changes during earthquake rupture, *Bull. Seism. Soc. Am.* **88,** 512–522.

Delouis, B., D. Giardini, P. Lundgren, and J. Salichon (2002). Joint inversion of InSAR, GPS, teleseismic, and strong-motion data for the spatial and temporal distribution of earthquake slip: application to the 1999 İzmit mainshock, *Bull. Seism. Soc. Am.* **92,** no. 1, 278–299.

Dieterich, J. D. (1981). Potential for geophysical experiments in large scale tests, *Geophys. Res. Lett.* **8,** 653–656.

Ellsworth, W. L., and G. C. Beroza (1995). Seismic evidence for a seismic nucleation phase, *Science* **268,** 851–855.

Felzer, K. R., and G. C. Beroza (1999). Deep structure of a fault discontinuity, *Geophys. Res. Lett.* **26,** 2121–2124.

Fumal, T. E., R. M. Langridge, H. D. Stenner, S. Christofferson, J. F. Dolan, R. Hartleb, T. Rockwell, T. Dawson, A. Z. Tucker, Z. Cakir, A. Dikbas, B. Yerli, and A. Barka (1999). Slip distribution and geometry of the Sakarya section of the 1999 İzmit earthquake ground rupture, western Turkey, *EOS, Trans. AGU* **80(17),** Fall Meeting supplement, F669.

Harris, R. A. (1998). Stress triggers, stress shadows, and implications for seismic hazard, introduction to the special issue, *J. Geophys. Res.* **103,** 24,347–24,358.

Harris, R. A., and S. M. Day (1993). Dynamics of fault interaction: parallel strike-slip faults, *J. Geophys. Res.* **98,** 4461–4472.

Harris, R. A., and S. M. Day (1999). Dynamic 3D simulations of earthquakes on en echelon faults, *Geophys. Res. Lett.* **26,** 2089–2092.

Harris, R. A., and R. W. Simpson (1998). Suppression of large earthquakes by stress shadows: a comparison of Coulomb and rate-and-state failure, *J. Geophys. Res.* **103,** 24,439–24,451.

Harris, R. A., R. J. Archuleta, and S. M. Day (1991). Fault steps and the dynamic rupture process: 2-d numerical simulations of a spontaneously propagating shear fracture, *Geophys. Res. Lett.* **18,** 893–896.

Hartleb, R. D., T. E. Dawson, A. Z. Tucker, J. F. Dolan, T. K. Rockwell, B. Yerli, A. Dikbas, Z. Cakir, T. Gurer, O. Uslu, and A. A. Barka (1999). Surface rupture and slip distribution along the Düzce strand of the 17-August-1999 İzmit, Turkey earthquake, *EOS, Trans. AGU* **80(17),** Fall Meeting supplement, F670.

Hartleb, R. D., J. F. Dolan, S. Akyuz, T. E. Dawson, B. Yerli, A. Z. Tucker, T. K. Rockwell, E. Toroman, Z. Cakir, A. Dikbas, and E. Altunel (2002). Surface rupture and slip distribution along the Karadere segment of the 17 August 1999 İzmit, Turkey, earthquake, *Bull. Seism. Soc. Am.*

Honkura, Y., A. M. Isikara, N. Oshiman, A. Ito, B. Ucer, S. Baris, M. Tuncer, M. Matsushima, R. Pektas, C. Celik, B. Tank, F. Takahashi, M. Nakanishi, R. Yoshimura, Y. Ikeda, and T. Komut (2000). Preliminary results of multidisciplinary observations before, during and after the Kocaeli (İzmit) earthquake in the western part of the North Anatolian fault zone, *Earth Planets Space* **52,** 293–298.

Hubert-Ferrari, A., A. Barka, E. Jacques, S. S. Nalbant, B. Meyer, R. Armijo, P. Tapponnier, and G. C. P. King (2000). Seismic hazard in the Marmara Sea region following the 17 August 1999 İzmit earthquake, *Nature* **404,** 269–273.

Husseini, M. I., D. B. Jovanovich, M. J. Randall, and L. B. Freund (1975). The fracture energy of earthquakes, *Geophys. J. R. Astr. Soc.* **43,** 367–385.

Ida, Y. (1972). Cohesive force across the tip of a longitudinal shear crack and Griffith's specific surface energy, *J. Geophys. Res.* **84,** 3796–3805.

Ito, A., B. Ucer, S. Baris, Y. Honkura, T. Kono, A. Nakamura, R. Pektas, Y. Ishikawa, and A. M. Isikara (1999). Precise distribution of aftershocks of the İzmit earthquake of August 17, 1999, Turkey, *EOS, Trans. AGU* **80(17),** Fall Meeting supplement, F662–663.

Kase, Y., and K. Kuge (1998). Numerical simulation of spontaneous rupture processes on two non-coplanar faults: the effect of geometry on fault interaction, *Geophys. J. Int.* **135,** 911–922.

Knuepfer, P. L. K. (1989). Implications of the characteristics of end-points of historical surface fault ruptures for the nature of fault segmentation, *U.S. Geol. Surv. Open-File Rept. 89-315*, 193–228.

Kusçu, I., M. Okamura, H. Matsuoka, S. Karagoz, and Y. Awata (2000). Active faults in the Gulf of İzmit, imaged by high-resolution seismic profiles, *EOS* **81,** F835.

Langridge, R. M., H. D. Stenner, T. E. Fumal, S. A. Christofferson, T. K. Rockwell, R. D. Hartleb, J. Bachhuber, and A. A. Barka (2002). Geometry, slip distribution, and kinematics of surface rupture on the Sakarya fault segment during the 17 August 1999 İzmit, Turkey, earthquake *Bull. Seism. Soc. Am.* **92,** no. 1, 107–125.

Lettis, W., J. Bachhuber, A. Barka, R. Witter, and C. Brankman (2000). Surface fault rupture and segmentation during the Kocaeli earthquake, in *The 1999 İzmit and Düzce Earthquakes: Preliminary Results*, A. Barka, Ö. Kozaci, S. Ayküz, and E. Altunel (Editors), Istanbul Technical University, Istanbul, Turkey, 31–54.

Li, Y.-G., J. E. Vidale, K. Aki, C. J. Marone, and W. H. K. Lee (1994). Fine structure of the Landers fault zone: segmentation and the rupture process, *Science* **265,** 367–370.

Magistrale, H., and S. Day (1999). 3D simulations of multi-segment thrust fault rupture, *Geophys. Res. Lett.* **26,** 2093–2096.

McGarr, A. (1984). Scaling of ground motion parameters, state of stress, and focal depth, *J. Geophys. Res.* **89,** 6969–6979.

Nalbant, S. S., A. Hubert, and G. C. P. King (1998). Stress coupling between earthquakes in northwest Turkey and the North Aegean sea, *J. Geophys. Res.* **103,** 24,469–24,486.

Okay, A. I., A. Kaslilar-Ozcan, C. Imren, A. Boztepe-Guney, E. Demirbag, and I. Kusçu (2000). Active faults and evolving strike-slip basins in the Marmara Sea, northwest Turkey: a multichannel seismic reflection study, *Tectonophysics* **321,** 189–218.

Parke, J. R., T. A. Minshull, G. Anderson, R. S. White, D. McKenzie, I. Kusçu, J. M. Bull, N. Gorur, and C. Sengor (1999). Active faults in the Sea of Marmara, western Turkey, imaged by seismic reflection profiles, *Terra Nova* **11,** 223–227.

Parsons, T., S. Toda, R. S. Stein, A. Barka, and J. Dieterich (2000). Heightened odds of large earthquakes near Istanbul: an interaction-based probability calculations, *Science* **288,** 661–665.

Reilinger, R. E., S. Ergintav, R. Bürgmann, S. McClusky, O. Lenk, A. Barka, O. Gurkan, L. Hearn, K. L. Feigl, R. Cakmak, B. Aktug, H. Ozener, and M. N. Toksöz (2000a). Coseismic and postseismic fault slip for the 17 August 1999, $M = 7.5$, İzmit, Turkey earthquake, *Science* **289,** 1519–1524.

Reilinger, R., N. Toksöz, S. McClusky, and A. Barka (2000b). 1999 İzmit, Turkey earthquake was no surprise, *GSA Today,* Vol. 10.

Segall, P., and D. D. Pollard (1980). Mechanics of discontinuous faults, *J. Geophys. Res.* **85,** 4337–4350.

Sibson, R. H. (1985). Stopping of earthquake ruptures at dilational fault jogs, *Nature* **316,** 248–251.

Sibson, R. H. (1986). Rupture interactions with fault jogs, in *Earthquake Source Mechanics,* Geophysical Monographs, Maurice Ewing Series 6, American Geophysical Union, 157–167.

Sieh, K. E., L. M. Jones, E. Hauksson, K. W. Hudnut, D. Eberhart-Phillips, T. H. Heaton, S. E. Hough, L. K. Hutton, H. Kanamori, *et al.* (1993). Near-field investigations of the Landers earthquake sequence, April to July 1992, *Science* **260,** 171–176.

Sowers, J. M., J. R. Unruh, W. R. Lettis, and T. D. Rubin (1994). Relationship of the Kickapoo fault to the Johnson Valley and Homestead Valley faults, San Bernardino County, California, *Bull. Seism. Soc. Am.* **84,** 528–536.

Stein, R. S., A. A. Barka, and J. H. Dieterich (1997). Progressive failure on the North Anatolian fault since 1939 by earthquake stress triggering, *Geophys. J. Int.* **128,** 594–604.

U.S. Geological Survey (2000). U.S. Geological Survey Circular 1193, Implications for earthquake risk reduction in the United States from the Kocaeli, Turkey, earthquake of August 17, 1999.

Wallace, R. E. (1970). Earthquake recurrence intervals of the San Andreas fault, *Geol. Soc. Am. Bull.* **81,** 2875–2890.

Wesnousky, S. G. (1988). Seismological and structural evolution of strike-slip faults, *Nature* **335,** 340–343.
Wright, T., E. Fielding, and B. Parsons (2001). Triggered slip: observations of the 17 August 1999 İzmit (Turkey) earthquake using radar interferometry, *Geophys. Res. Lett.* **28,** 1079–1082.

U.S. Geological Survey
Menlo Park, California
(R.A.H.)

University of Southern California
Los Angeles, California
(J.F.D., R.H.)

San Diego State University
San Diego, California
(S.M.D.)

Manuscript received 30 August 2000.